Supplement of Atmos. Chem. Phys., 24, 1315–1328, 2024
https://doi.org/10.5194/acp-24-1315-2024-supplement

Atmospheric Chemistry and Physics
Open Access
EGU

Supplement of

Analysis of atmospheric particle growth based on vapor concentrations measured at the high-altitude GAW station Chacaltaya in the Bolivian Andes

Arto Heitto et al.

Correspondence to: Arto Heitto (arto.heitto@uef.fi) and Cheng Wu (cheng.wu@gu.se)

Sensitivity of Iodide CIMS to organics

Iodide CIMS sensitivity to organics has been described in previous studies (Lee, et al. 2014; Lopez-Hilfiker, et al. 2016). It is normally reported as normalized sensitivity to a million total reagent ion counts per second (cps). These normalized sensitivity values depend on instrument parameters, including inlet and IMR temperature and pressure, and electric fields. The latter determines the transmission efficiency and decluttering strength.

As described in Eq. (1), there are two main components, production ion formation and transmission, which decide the sensitivity (Lopez-Hilfiker, et al. 2016):

$$S_i = \int_0^t k_f[I^-] \times T^i\left(\frac{m}{Q}, B^i\right) \quad (1)$$

Where S_i is the sensitivity observed for reaction time t, k_f is the production ion formation rate constant, $[I^-]$ is the concentration of the reagent ions in the IMR, and T^i is the ion-specific transmission efficiency, which depends on the mass-to-charge (m/Q) and the adduction ion binding energy (B^i).

The changes in the IMR pressure, the iodide flow (F_{iodide}), and the sampling flow (F_{sampling}) do not affect the transmission, but the production ion formation by varying t and $[I^-]$. The changes in $[I^-]$ would be canceled out by the normalization to the concentration of reagent ion. The reaction time t can be calculated as the time of total volumetric flow (including iodide flow and inlet flow, $F_{\text{iodide}} + F_{\text{sampling}}$, in slpm) takes to sweep the physical volume of the IMR (V_{IMR}) at given pressure P_{IMR} adjusted to P_0 = 1bar.

$$t = \frac{V_{IMR}}{(F_{\text{iodide}}+F_{\text{sampling}})\frac{P_0}{P_{\text{IMR}}}} \quad (2)$$

A correction factor could be calculated based on the changes in t:

$$\text{correction factor 1} = \frac{t}{t^S} = \frac{(F^S_{\text{iodide}}+F^S_{\text{sampling}})*P_{\text{IMR}}}{(F_{\text{iodide}}+F_{\text{sampling}})*P^S_{\text{IMR}}} \quad (3)$$

where t^S is the reaction time with the standard setting, F^S_{iodide} and F^S_{sampling} are the iodide flow and sampling flow with the standard setting, and P^S_{IMR} is the IMR pressure with the standard setting. F^S_{iodide} = 2 slpm, F^S_{sampling} = 2 slpm, P^S_{IMR} = 100 mbar.

On the top of the correction based on Eqs. (1), (2) and (3), sensitivity changes also due to the dilution of the sampling flow in the IMR by the reagent ion flow ($F_{\text{sampling}}/(F_{\text{Iodide}} + F_{\text{sampling}})$), which is corrected by another factor:

$$\text{correction factor 2} = \frac{F_{\text{sampling}}(F^S_{\text{iodide}}+F^S_{\text{sampling}})}{F^S_{\text{sampling}}(F_{\text{Iodide}}+F_{\text{sampling}})} \quad (4)$$

Model simulations considering the changes in air mass

A sharp increase in organic vapor or/and particle concentration during the day may be an implication of change in the air mass. In these situations our model cannot capture correctly the processes affecting the changes in the particle size. For these cases, in addition to the simulations presented in the main text, we tried to predict how particle size would have evolved in the original airmass, by assuming that particles observed after and before the high concentration period are both from the original air mass. For this, the concentrations of organics were approximated by using a linear interpolation between measurements right before and after the air mass change (Fig. S6 a-b). However, for sulfuric acid this approach was not applicable since it has a strong diurnal variation. Instead, assumption was made that sulfuric acid concentrations follow a Gaussian curve during daytime and a similar method to fill in the "missing" data was

applied as explained in Section 2.2 for gaps in sulfuric acid data. For temperature and RH, the measured values throughout these simulations were used. The temperature did have a diurnal variation, but it is more governed by sunlight and other meteorological conditions than air mass. For RH, no any clear pattern was identified that would have allowed a prediction how it behaves. Also, temperature and RH have only a minor effect on the simulated growth.

Figure S5 c-d presents these simulations for two NPF days in May with air mass change. In these cases, the changes in size distribution and organic vapor concentrations suggested that the air mass impacting the station changed after the event started, and again after few hours, possibly changed back to the original air mass. In April, similar analyses were not possible for the NPFs with inhomogeneous air masses since the growth was not seen after the second air mass change in the afternoon. In addition, the changes in organic vapor concentrations were smaller in April (no change in ELVOC concentration, for LVOC concentrations less than 30 % increase) than in May during air mass changes, suggesting that this kind of model simulation would not differ substantially from the base case simulation, i.e. from the simulation where changes in air mass have not been taken into account.

The results show, that in the original air mass, the particles may grow substantially slower compared to the measured particles. However, any definite conclusions are hard to make, since only ensemble particle population is available from the measurements.

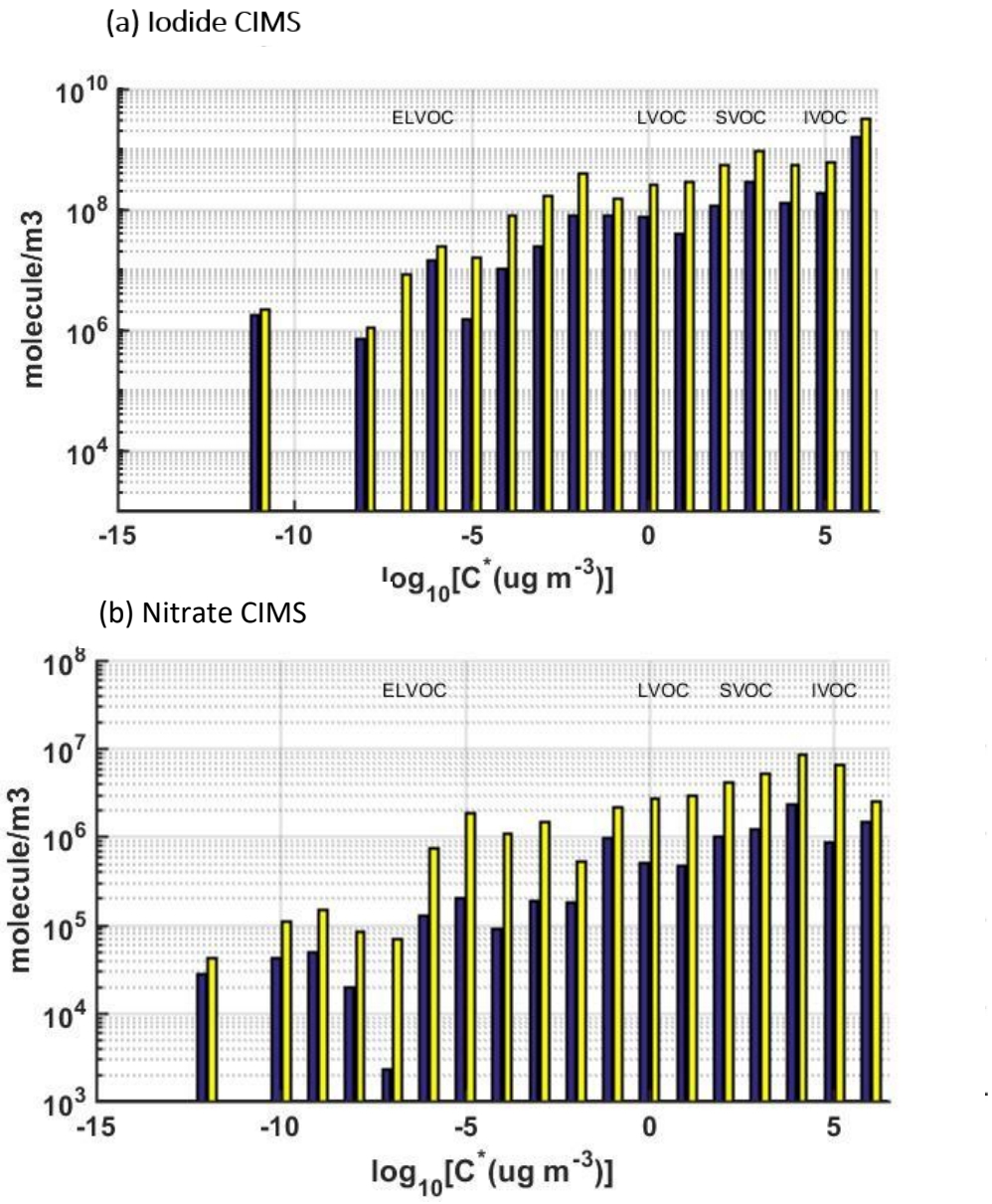

Figure S1 Volatility distributions in the form of VBS as derived from the gas phase molecular composition detected by FIGAERO Iodide CIMS (a) and Nitrate CIMS (b) from two typical events: one without (dark blue) and one with substantial urban influence (yellow).

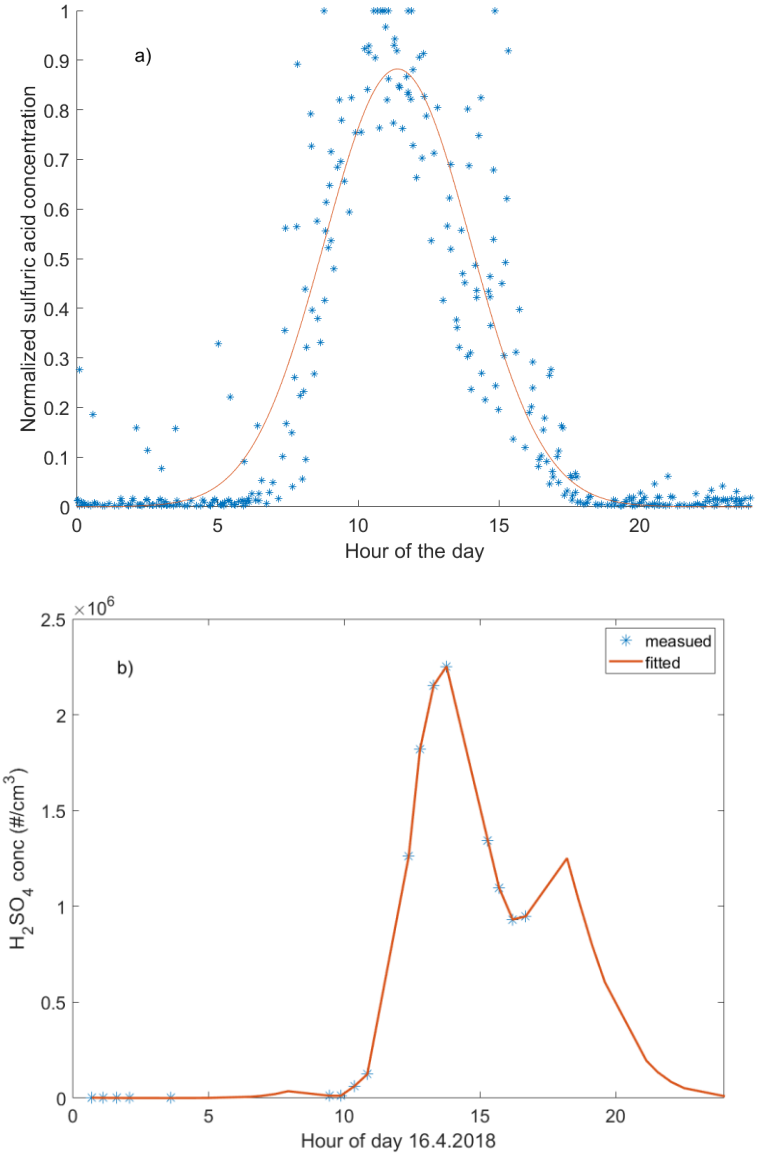

Figure S2. a) Normalized sulfuric acid measurements for days in May with assumed homogeneous air mass and gaussian curve fitted to them. b) Measured sulfuric acid concentrations on 16.4. (blue stars) and the concentration used as an input for the model (red line). The latter is based on measured data when available (approx. 10 am to 4 pm) and the Gaussian distribution presented with amplitude normalized based on the measured data.

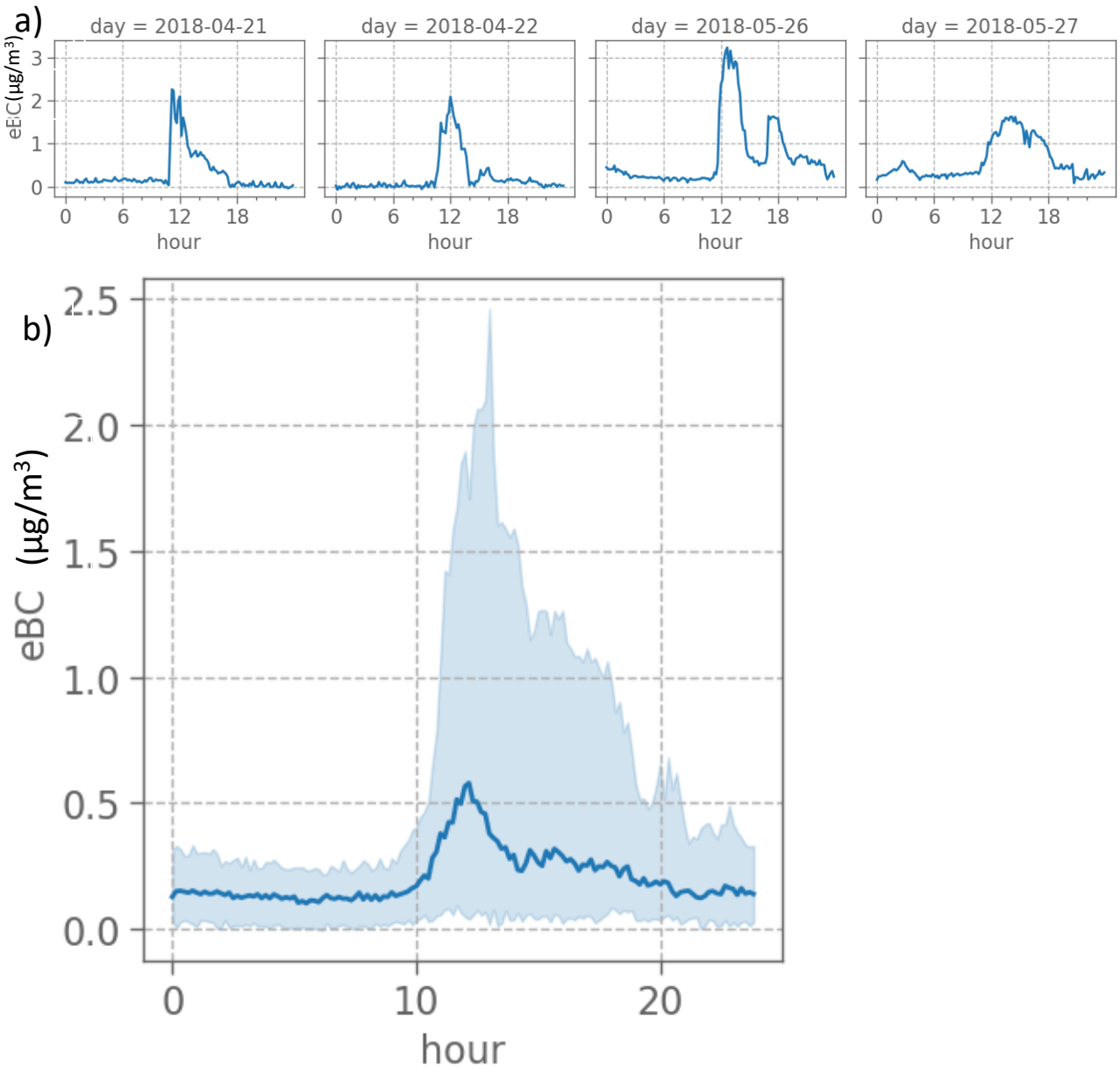

Figure S3. a) Black carbon concentration (eBC) on Chacaltaya station on a) analyzed days with assumed inhomogeneous air mass. b) Median diurnal cycle of black carbon concentration during the SALTENA campaign (blue line). The light blue shaded area in b presents 25–75 % quantile range.

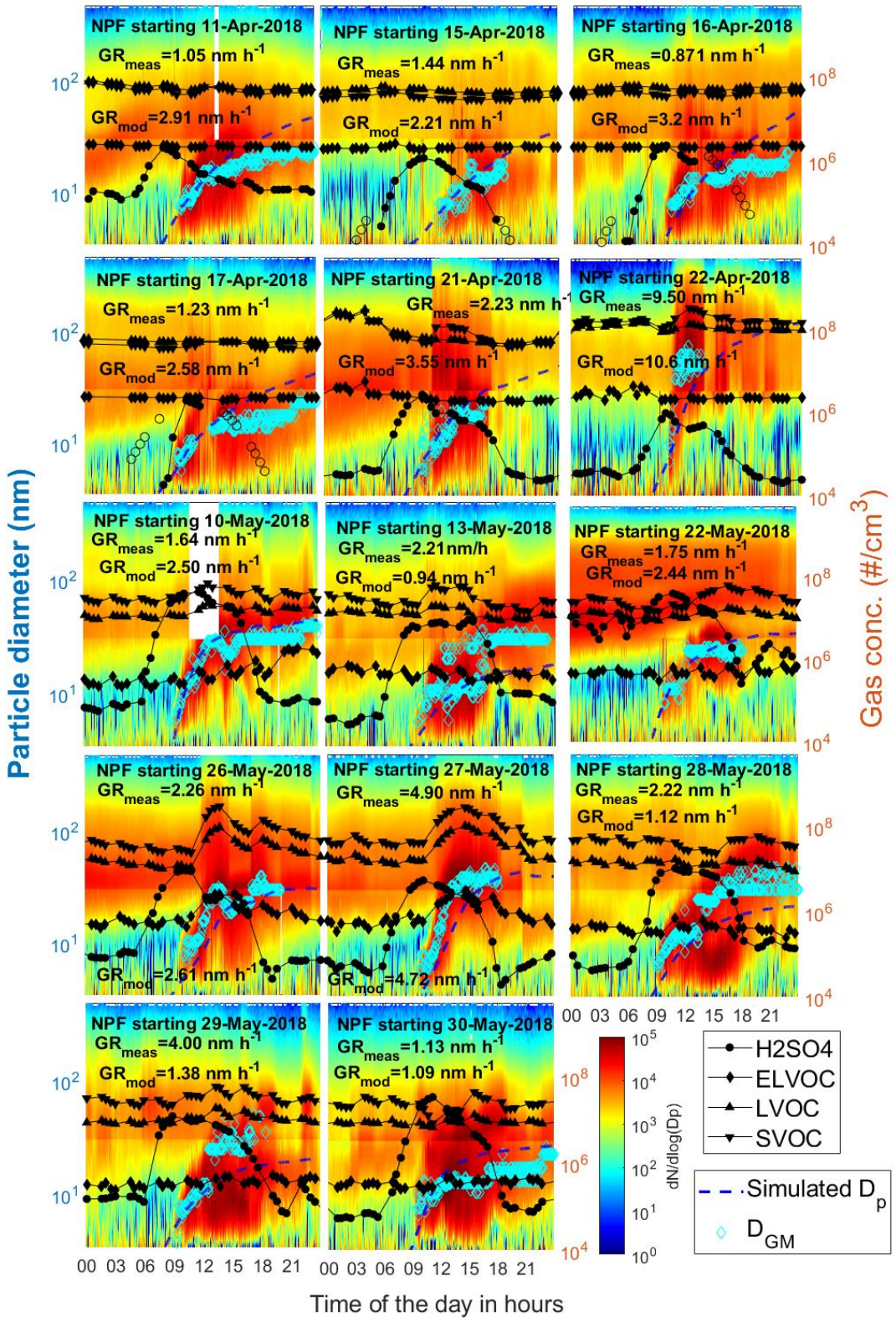

Figure S4 Modelled particle growth, measured gas-phase concentrations of organics and sulfuric acid, and measured particle size distribution as a function of time for all days analyzed in the study. The particle diameter for the measured size distribution, fitted geometric mean diameters of nucleation mode and modelled particle growth is on left y-axis. Gas concentrations are on y-axis on right.

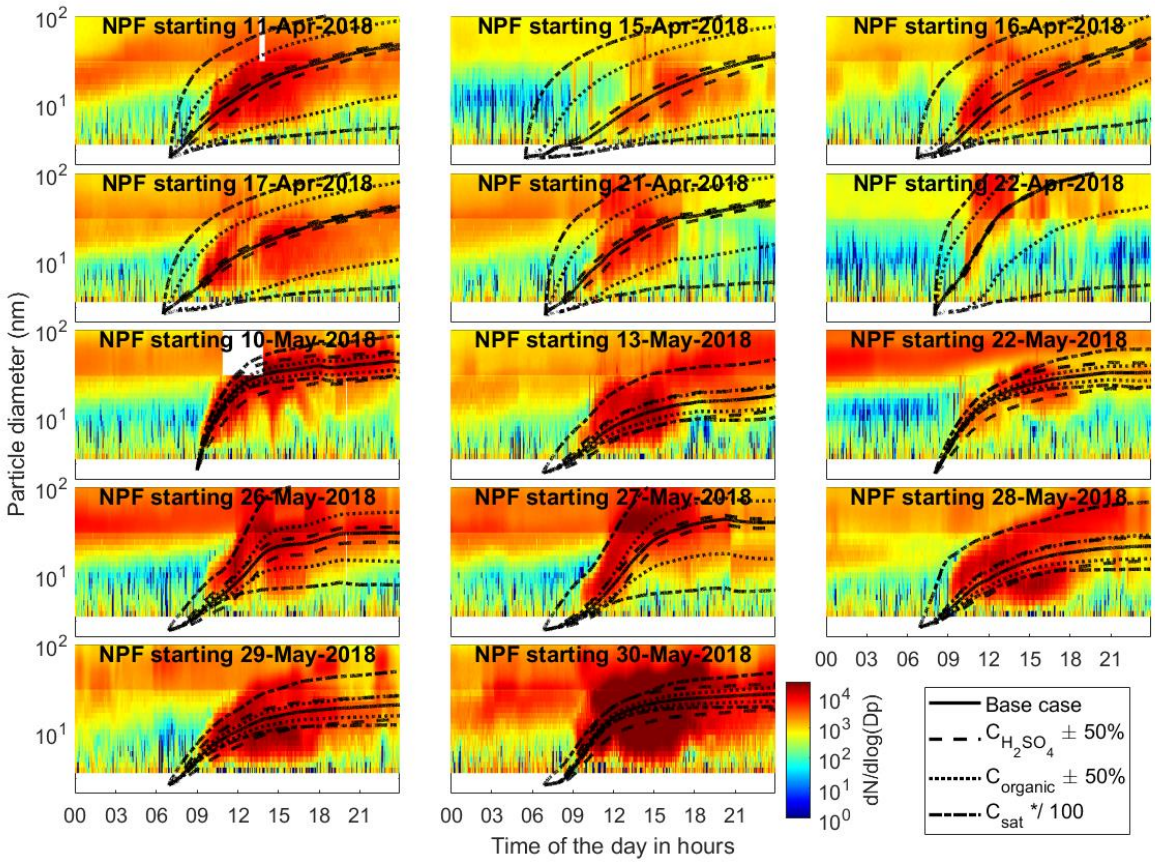

Figure S5 Sensitivity tests of modelled particle growth for sulfuric acid concentrations (± 50 %), organic vapor concentrations (± 50 %) and saturation vapor concentrations of organics (multiplied or divided by a factor of 100).

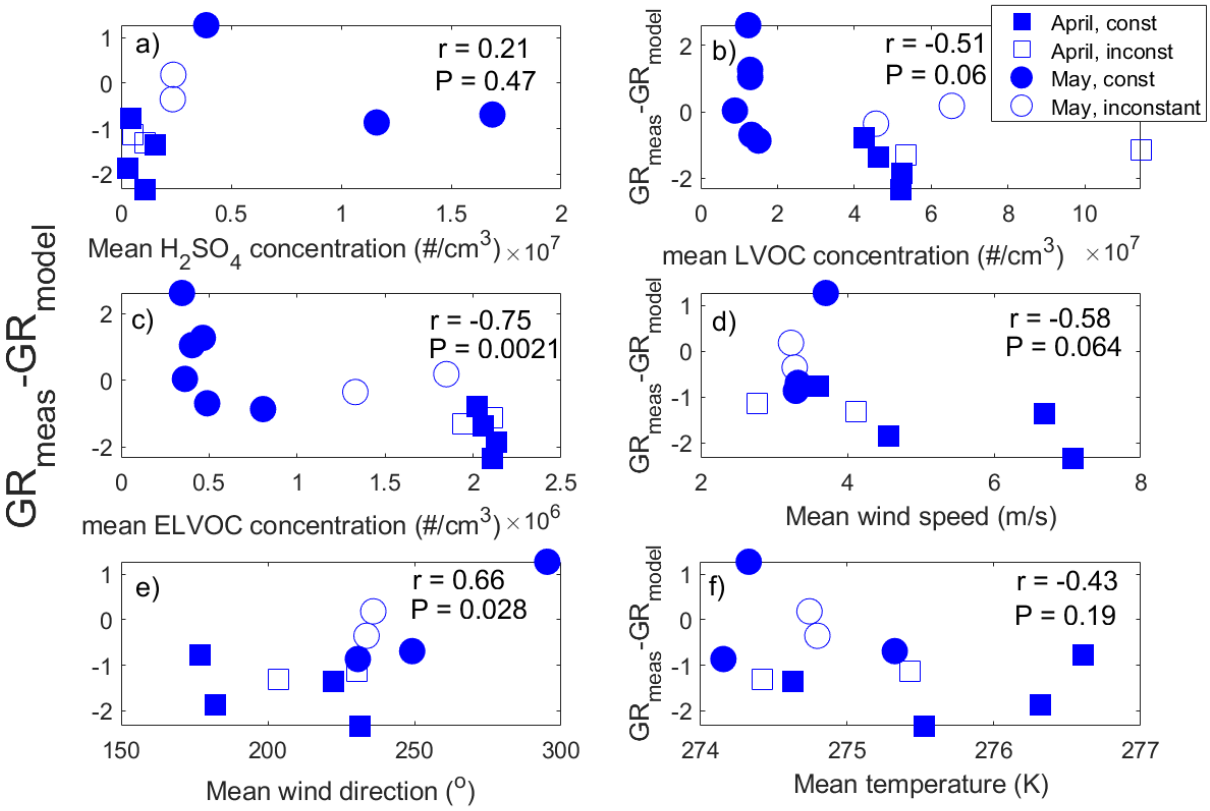

Figure S6. Absolute difference of measured and modelled particle growth as a function of mean a) sulfuric acid concentration, b) LVOC concentration, c) ELVOC concentrations, d) wind speed, e) wind direction, and f) temperature. Data from April and May are shown with squares and circles, respectively. The cases where air masses were estimated to be fairly homogeneous throughout the growth event are shown with filled markers and the cases where changes in air mass were assumed to affect the particle size distribution evolution are shown with empty markers.

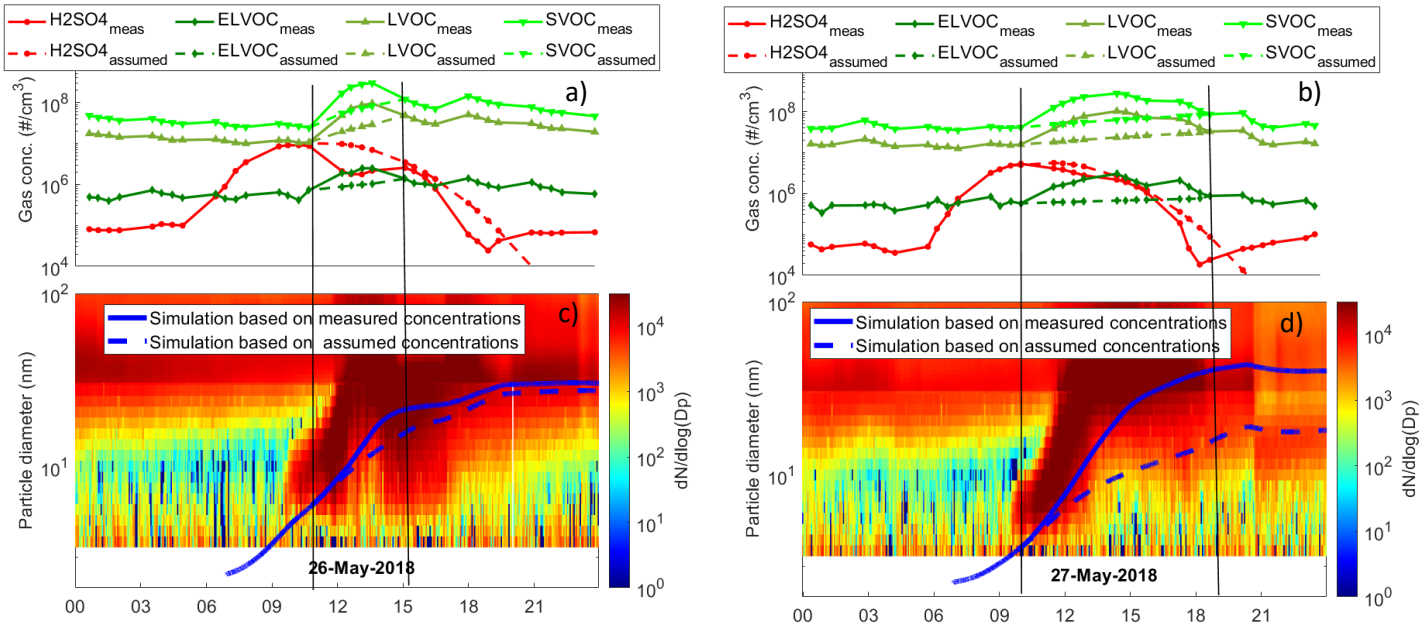

Figure S7. a) – b) Measured vapor concentrations (solid lines with markers) and assumed background concentrations (dashed lines with markers) of organics and sulfuric acid over air mass change as a function of time for 26th and 27th of May 2018, respectively. c) – d) Simulated particle growth based on measured and assumed vapor concentrations of organics and sulfuric acid as a function of time compared to the measured particle size distribution for 26th and 27th of May 2018. The black vertical lines indicate assumed time period where the air mass was different related to the air mass at the beginning of the NPF event.

Table S1. Summary of the data for the analyzed NPF events.

Date	start time (t_s)	end time (t_e)	Geometric mean diameter at t_s (nm)	Geometric mean diameter at t_e (nm)	mean H_2SO_4 concentration (#/cm^3)	mean ELVOC concentration (#/cm^3)	mean LVOC concentration (#/cm^3)	mean SVOC concentration (#/cm^3)	events during day	Assumed homogeneous air mass
11.4.	9:51 11.4.	2:57 12.4.	7.3	30	$0.031 * 10^7$	$0.21 * 10^7$	$5.2 * 10^7$	$4.4 * 10^7$	1	yes
15.4.	11:55 15.4.	18:37 15.4.	6.0	14	$0.044 * 10^7$	$0.20 * 10^7$	$4.3 * 10^7$	$2.9 * 10^7$	1	yes
16.4.	10:12 16.4.	22:41 16.4.	6.9	23	$0.11 * 10^7$	$0.21 * 10^7$	$5.2 * 10^7$	$3.9 * 10^7$	1	yes
17.4.	9:29 17.4.	2:59 18.4.	6.0	30	$0.15 * 10^7$	$0.21 * 10^7$	$4.6 * 10^7$	$3.8 * 10^7$	1	yes
21.4.	9:51 21.4.	16:33 21.4.	6.0	23	$0.11 * 10^7$	$0.19 * 10^7$	$5.4 * 10^7$	$7.8 * 10^7$	1	no
22.4.	10:10 22.4.	13:47 22.4.	7.0	51	$0.054 * 10^7$	$0.21 * 10^7$	$11 * 10^7$	$24 * 10^7$	1	no
10.5.	8:51 10.5.	2:56 11.5.	4.1	39	$1.2 * 10^7$	$0.081 * 10^7$	$1.5 * 10^7$	$3.9 * 10^7$	2	yes
13.5.	9:35 13.5.	23:07 13.5.	5.6	30	$0.39 * 10^7$	$0.046 * 10^7$	$1.3 * 10^7$	$3.2 * 10^7$	2	yes
22.5.	9:57 22.5.	18:14 22.5.	7.7	23	$1.7 * 10^7$	$0.048 * 10^7$	$1.3 * 10^7$	$3.7 * 10^7$	2	yes
26.5.	10:05 26.5.	19:56 26.5.	7.7	30	$0.23 * 10^7$	$0.13 * 10^7$	$4.6 * 10^7$	$13 * 10^7$	1	no
27.5.	9:49 27.5.	18:06 27.5.	6.0	33	$0.24 * 10^7$	$0.18 * 10^7$	$6.5 * 10^7$	$18 * 10^7$	1	no
28.5.	9:02 28.5.	00:05 29.5.	6.3	46	$0.39 * 10^7$	$0.040* 10^7$	$1.3 * 10^7$	$3.9 * 10^7$	2	yes
29.5.	9:18 29.5.	18:24 29.5.	3.7	48	$0.56 * 10^7$	$0.035 * 10^7$	$1.2 * 10^7$	$4.0 * 10^7$	2	yes
30.5.	9:24 30.5.	2:57 31.5.	7.7	30	$0.75 * 10^7$	$0.036 * 10^7$	$0.89 * 10^7$	$2.3 * 10^7$	2	yes

References

Lee, B. H., Lopez-Hilfiker, F. D., Mohr, C., Kurtén, T., Worsnop, D. R., and Thornton, J. A.: An iodide-adduct high-resolution time-of-flight chemical-ionization mass spectrometer: Application to atmospheric inorganic and organic compounds, Environ. Sci. Technol., 48, 6309–6317, https://doi.org/10.1021/es500362a, 2014.

Lopez-Hilfiker, F. D., Iyer, S., Mohr, C., Lee, B. H., D'Ambro, E. L., Kurtén, T., and Thornton, J. A.: Constraining the sensitivity of iodide adduct chemical ionization mass spectrometry to multifunctional organic molecules using the collision limit and thermodynamic stability of iodide ion adducts, Atmos. Meas. Tech., 9, 1505–1512, https://doi.org/10.5194/amt-9-1505-2016, 2016.